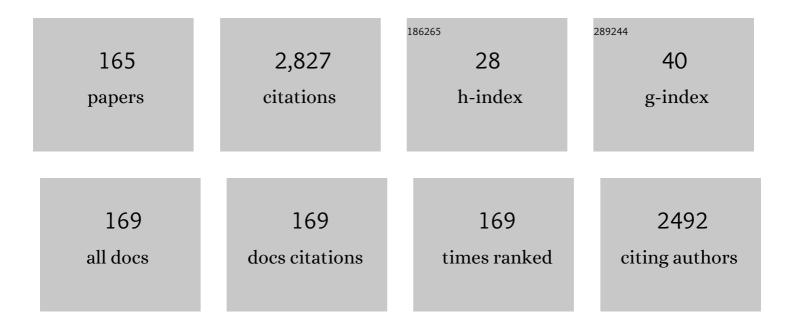
List of Publications by Year in descending order

Source: https://exaly.com/author-pdf/3700757/publications.pdf Version: 2024-02-01



#	Article	IF	CITATIONS
1	Materials science aspects of zinc–air batteries: a review. Materials for Renewable and Sustainable Energy, 2014, 3, 1.	3.6	186
2	Evaluation of erosion–corrosion in multiphase flow via CFD and experimental analysis. Wear, 2003, 255, 237-245.	3.1	106
3	Electrodeposition of Zn–Mn alloys in the presence of thiocarbamide. Surface and Coatings Technology, 2002, 154, 294-303.	4.8	63
4	Electrochemical oxidation of WC in acidic sulphate solution. Corrosion Science, 2004, 46, 453-469.	6.6	50
5	Spatio-temporal organization in alloy electrodeposition: a morphochemical mathematical model and its experimental validation. Journal of Solid State Electrochemistry, 2013, 17, 467-479.	2.5	48
6	A SERS Investigation of Cyanide Adsorption and Reactivity during the Electrodeposition of Gold, Silver, and Copper from Aqueous Cyanocomplexes Solutions. Journal of Physical Chemistry C, 2008, 112, 6352-6358.	3.1	45
7	Turing pattern formation on the sphere for a morphochemical reaction-diffusion model for electrodeposition. Communications in Nonlinear Science and Numerical Simulation, 2017, 48, 484-508.	3.3	43
8	In Operando Photoelectrochemical Femtosecond Transient Absorption Spectroscopy of WO <sub>3</sub> /BiVO <sub>4</sub> Heterojunctions. ACS Energy Letters, 2019, 4, 2213-2219.	17.4	42
9	A SERS investigation of the electrodeposition of Ag–Au alloys from free-cyanide solutions. Journal of Electroanalytical Chemistry, 2004, 563, 133-143.	3.8	39
10	Electrosynthesis of Co/PPy nanocomposites for ORR electrocatalysis: a study based on quasi-in situ X-ray absorption, fluorescence and in situ Raman spectroscopy. Electrochimica Acta, 2014, 137, 535-545.	5.2	39
11	An in Situ Synchrotron-Based Soft X-ray Microscopy Investigation of Ni Electrodeposition in a Thin-Layer Cell. Journal of Physical Chemistry C, 2009, 113, 9783-9787.	3.1	38
12	Spatio-temporal organization in a morphochemical electrodeposition model: Hopf and Turing instabilities and their interplay. European Journal of Applied Mathematics, 2015, 26, 143-173.	2.9	38
13	Magnetic field effects on the initial stages of electrodeposition processes. Journal of Electroanalytical Chemistry, 2008, 615, 191-196.	3.8	37
14	Nucleation and growth of thin nickel layers under the influence of a magnetic field. Journal of Electroanalytical Chemistry, 2009, 626, 174-182.	3.8	37
15	Fabrication of a Sealed Electrochemical Microcell for in Situ Soft X-ray Microspectroscopy and Testing with in Situ Co-Polypyrrole Composite Electrodeposition for Pt-Free Oxygen Electrocatalysis. Analytical Chemistry, 2014, 86, 664-670.	6.5	37
16	Weakly nonlinear analysis of Turing patterns in a morphochemical model for metal growth. Computers and Mathematics With Applications, 2015, 70, 1948-1969.	2.7	36
17	An SFG/DFG investigation of CNâ^' adsorption at an Au electrode in 1-butyl-1-methyl-pyrrolidinium bis(trifluoromethylsulfonyl) amide ionic liquid. Electrochemistry Communications, 2010, 12, 56-60.	4.7	35
18	Electrochemical dynamics and structure of the Ag/AgCl interface in chloride-containing aqueous solutions. Surface and Coatings Technology, 2007, 201, 4619-4627.	4.8	34

#	Article	IF	CITATIONS
19	A novel polymeric leveller for the electrodeposition of copper from acidic sulphate bath: A spectroelectrochemical investigation. Electrochimica Acta, 2007, 52, 4767-4777.	5.2	34
20	In situ soft X-ray dynamic microscopy of electrochemical processes. Electrochemistry Communications, 2008, 10, 1680-1683.	4.7	34
21	Numerical approximation of Turing patterns in electrodeposition by ADI methods. Journal of Computational and Applied Mathematics, 2012, 236, 4132-4147.	2.0	33
22	Electrodeposition of yttria/cobalt oxide and yttria/gold coatings onto ferritic stainless steel for SOFC interconnects. Journal of Power Sources, 2010, 195, 4772-4778.	7.8	32
23	Numerical issues related to the modelling of electrochemical impedance data by non-linear least-squares. International Journal of Non-Linear Mechanics, 2005, 40, 557-570.	2.6	31
24	Localised corrosion processes of austenitic stainless steel bipolar plates for polymer electrolyte membrane fuel cells. Journal of Power Sources, 2010, 195, 3590-3596.	7.8	31
25	An in situ SFG and SERS investigation into the electrodeposition of Au from and solutions. Journal of Electroanalytical Chemistry, 2007, 602, 61-69.	3.8	30
26	Characterization of the particulate anode of a laboratory flow Zn–air fuel cell. Journal of Applied Electrochemistry, 2017, 47, 877-888.	2.9	30
27	An SFG investigation of Au(111) and Au(210) electrodes in aqueous solutions containing KCN and cetylpyridinium chloride. Journal of Electroanalytical Chemistry, 2004, 574, 85-94.	3.8	29
28	Soft Xâ€ray Imaging and Spectromicroscopy: New Insights in Chemical State and Morphology of the Key Components in Operating Fuel ells. Chemistry - A European Journal, 2012, 18, 10196-10210.	3.3	29
29	Mass-transport effects on texture formation of nickel electrodeposits. Materials Chemistry and Physics, 2000, 66, 278-285.	4.0	28
30	Voltammetric and in situ FTIRS study on CNâ^' and Au(CN)â^'x complexes at the polycrystalline gold surface in citrate medium. Journal of Electroanalytical Chemistry, 2004, 569, 53-60.	3.8	28
31	Electrodeposition of Cu from acidic sulphate solutions containing cetyltrimethylammonium bromide (CTAB). Journal of Applied Electrochemistry, 2008, 38, 1561-1569.	2.9	28
32	Doubly Resonant Sum Frequency Generation Spectroscopy of Adsorbates at an Electrochemical Interface. Journal of Physical Chemistry C, 2008, 112, 11791-11795.	3.1	27
33	Metallic Plate Corrosion and Uptake of Corrosion Products by Nafion in Polymer Electrolyte Membrane Fuel Cells. ChemSusChem, 2010, 3, 846-850.	6.8	27
34	Electrodeposition and pyrolysis of Mn/polypyrrole nanocomposites: a study based on soft X-ray absorption, fluorescence and photoelectron microspectroscopies. Journal of Materials Chemistry A, 2015, 3, 19155-19167.	10.3	26
35	Effects of Tl on the electrocrystallisation of thick Au layers from KAu(CN)2 solutions. Journal of Crystal Growth, 2002, 243, 190-203.	1.5	25
36	Coupling of Morphology and Chemistry Leads to Morphogenesis in Electrochemical Metal Growth: A Review of the Reaction-Diffusion Approach. Acta Applicandae Mathematicae, 2012, 122, 53.	1.0	25

#	Article	IF	CITATIONS
37	In-situ photoelectron microspectroscopy during the operation of a single-chamber SOFC. Electrochemistry Communications, 2012, 24, 104-107.	4.7	25
38	In situ spectroelectrochemical measurements during the electro-oxidation of ethanol on WC-supported Pt-black, based on sum-frequency generation spectroscopy. Journal of Power Sources, 2010, 195, 4119-4123.	7.8	24
39	Electrodeposition of manganese oxide from eutectic urea/choline chloride ionic liquid: An in situ study based on soft X-ray spectromicroscopy and visible reflectivity. Journal of Power Sources, 2012, 211, 71-76.	7.8	23
40	Electrochemical fabrication of nanoporous gold-supported manganese oxide nanowires based on electrodeposition from eutectic urea/choline chloride ionic liquid. Electrochimica Acta, 2013, 87, 918-924.	5.2	23
41	In-situ Photoelectron Microspectroscopy and Imaging of Electrochemical Processes at the Electrodes of a Self-driven Cell. Scientific Reports, 2013, 3, 2848.	3.3	22
42	Highâ€lateral resolution Xâ€ray fluorescence microspectroscopy and dynamic mathematical modelling as tools for the study of electrodeposited electrocatalysts. X-Ray Spectrometry, 2015, 44, 263-275.	1.4	22
43	Electrodeposition of white gold alloys: an electrochemical, spectroelectrochemical and structural study of the electrodeposition of Au-Sn alloys in the presence of 4-cyanopyridine. Journal of Solid State Electrochemistry, 2004, 8, 147-158.	2.5	21
44	Spatio-Temporal Organization in a Morphochemical Electrodeposition Model: Analysis and Numerical Simulation of Spiral Waves. Acta Applicandae Mathematicae, 2014, 132, 377-389.	1.0	21
45	Corrosion of cemented carbide grades in petrochemical slurries. Part I - Electrochemical adsorption of CNÂ <sup>-</sup> , SCNÂ <sup>-</sup> and MBT: A study based on in situ SFG. International Journal of Refractory Metals and Hard Materials, 2016, 60, 37-51.	3.8	21
46	Parameter estimation for a morphochemical reaction-diffusion model of electrochemical pattern formation. Inverse Problems in Science and Engineering, 2019, 27, 618-647.	1.2	21
47	A SERS investigation of the electrodeposition of Ag–Au alloys from free-cyanide solutions – part II. Journal of Electroanalytical Chemistry, 2004, 570, 29-34.	3.8	20
48	An in situ near-ambient pressure X-ray Photoelectron Spectroscopy study of Mn polarised anodically in a cell with solid oxide electrolyte. Electrochimica Acta, 2015, 174, 532-541.	5.2	20
49	Electrodeposition of Mn-Co/Polypyrrole Nanocomposites: An Electrochemical and In Situ Soft-X-ray Microspectroscopic Investigation. Polymers, 2017, 9, 17.	4.5	20
50	Morphological spatial patterns in a reaction diffusion model for metal growth. Mathematical Biosciences and Engineering, 2010, 7, 237-258.	1.9	19
51	Corrosion of Ni in 1-butyl-1-methyl-pyrrolidinium bis (trifluoromethylsulfonyl) amide room-temperature ionic liquid: an in situ X-ray imaging and spectromicroscopy study. Physical Chemistry Chemical Physics, 2011, 13, 7968.	2.8	19
52	Inâ€Situ Xâ€Ray Spectromicroscopy Investigation of the Material Stability of SOFC Metal Interconnects in Operating Electrochemical Cells. ChemSusChem, 2011, 4, 1099-1103.	6.8	19
53	An investigation into the corrosion of Ag coins from the Greek colonies of Southern Italy. Part I: An in situ FT-IR and ERS investigation of the behaviour of Ag in contact with aqueous solutions containing 4-cyanopyridine. Corrosion Science, 2006, 48, 193-208.	6.6	18
54	Electrodeposition and Ageing of Mnâ€Based Binary Composite Oxygen Reduction Reaction Electrocatalysts. ChemElectroChem, 2015, 2, 1541-1550.	3.4	18

#	Article	IF	CITATIONS
55	Spectroelectrochemical investigation of the anodic and cathodic behaviour of zinc in 5.3ÂM KOH. Journal of Applied Electrochemistry, 2015, 45, 43-50.	2.9	18
56	Electrochemical fabrication of nanoporous gold decorated with manganese oxide nanowires from eutectic urea/choline chloride ionic liquid. Part III â^' Electrodeposition of Au–Mn: a study based on in situ Sum-Frequency Generation and Raman spectroscopies. Electrochimica Acta, 2016, 218, 208-215.	5.2	18
5 <b>7</b>	Experience with a pilot plant for the electrodeposition of Zn-Mn on wire. Transactions of the Institute of Metal Finishing, 1998, 76, 171-178.	1.3	17
58	Travelling waves in a reaction-diffusion model for electrodeposition. Mathematics and Computers in Simulation, 2011, 81, 1027-1044.	4.4	17
59	Electrodeposition of Au from [EMIm][TFSA] room-temperature ionic liquid: An electrochemical and Surface-Enhanced Raman Spectroscopy study. Journal of Electroanalytical Chemistry, 2011, 651, 1-11.	3.8	17
60	A study of external magnetic-field effects on nickel–iron alloy electrodeposition, based on linear and non-linear differential AC electrochemical response measurements. Journal of Electroanalytical Chemistry, 2011, 651, 197-203.	3.8	17
61	Quasi-in-Situ Single-Grain Photoelectron Microspectroscopy of Co/PPy Nanocomposites under Oxygen Reduction Reaction. ACS Applied Materials & Interfaces, 2014, 6, 19621-19629.	8.0	17
62	Morphological Evolution of Zn-Sponge Electrodes Monitored by In Situ X-ray Computed Microtomography. ACS Applied Energy Materials, 2020, 3, 4931-4940.	5.1	17
63	A non-linear AC spectrometry study of the electrodeposition of Cu from acidic sulphate solutions in the presence of PEG. Journal of Applied Electrochemistry, 2006, 36, 983-989.	2.9	16
64	Numerical modelling of MCFC cathode degradation in terms of morphological variations. International Journal of Hydrogen Energy, 2011, 36, 10403-10413.	7.1	16
65	Shedding light on electrodeposition dynamics tracked in situ via soft X-ray coherent diffraction imaging. Nano Research, 2016, 9, 2046-2056.	10.4	16
66	Cross-diffusion effects on a morphochemical model for electrodeposition. Applied Mathematical Modelling, 2018, 57, 492-513.	4.2	16
67	Electrodeposition of Co/CoO nanoparticles onto graphene for ORR electrocatalysis: a study based on micro-X-ray absorption spectroscopy and X-ray fluorescence mapping. Acta Chimica Slovenica, 2014, 61, 263-71.	0.6	16
68	Hydrodynamic problems related to the electrodeposition of AuCu/B4C composites. Electrochimica Acta, 2000, 45, 3431-3438.	5.2	15
69	Silver electrodeposition from water–acetonitrile mixed solvents and mixed electrolytes in the presence of tetrabutylammonium perchlorate. Part l—electrochemical nucleation on glassy carbon electrode. Journal of Solid State Electrochemistry, 2009, 13, 1577-1584.	2.5	15
70	Investigation of Au electrodeposition from [BMP][TFSA] room-temperature ionic liquid containing K[Au(CN)2] by in situ two-dimensional sum frequency generation spectroscopy. Journal of Electroanalytical Chemistry, 2011, 661, 20-24.	3.8	15
71	Electrochemical behaviour and surface characterisation of Zr exposed to an SBF solution containing glycine, in view of dental implant applications. Journal of Materials Science: Materials in Medicine, 2011, 22, 193-200.	3.6	15
72	Electrodeposition of nanostructured bioactive hydroxyapatite-heparin composite coatings on titanium for dental implant applications. Journal of Materials Science: Materials in Medicine, 2014, 25, 1425-1434.	3.6	15

#	Article	IF	CITATIONS
73	<i>In situ</i> soft x-ray fluorescence and absorption microspectroscopy: A study of Mn-Co/polypyrrole electrodeposition. Journal of Vacuum Science and Technology A: Vacuum, Surfaces and Films, 2015, 33, .	2.1	15
74	Coelectrodeposition of Ternary Mn-Oxide/Polypyrrole Composites for ORR Electrocatalysts: A Study Based on Micro-X-ray Absorption Spectroscopy and X-ray Fluorescence Mapping. Energies, 2015, 8, 8145-8164.	3.1	15
75	ORR stability of Mn–Co/polypyrrole nanocomposite electrocatalysts studied by quasi in-situ identical-location photoelectron microspectroscopy. Electrochemistry Communications, 2016, 69, 50-54.	4.7	15
76	Raman Spectroscopy of Organic Species Incorporated into Electrodeposited Gold Layers. Transactions of the Institute of Metal Finishing, 2002, 80, 25-28.	1.3	14
77	Prediction of Morphological Properties of Smart-Coatings for Cr Replacement, Based on Mathematical Modelling. Advanced Materials Research, 0, 138, 93-106.	0.3	14
78	In situ X-ray spectromicroscopy study of bipolar plate material stability for nano-fuel-cells with ionic-liquid electrolyte. Microelectronic Engineering, 2011, 88, 2456-2458.	2.4	14
79	An Electrochemical and Spectroelectrochemical Study of the Electrodeposition of Au from KAU(CN) <sub>2</sub> Solutions containing 4-Cyanopyridine and Cetylpyridinium Chloride. Transactions of the Institute of Metal Finishing, 2003, 81, 59-67.	1.3	13
80	Electrochemical adsorption of cyanide on Ag(111) in the presence of cetylpyridinium chloride. Journal of Crystal Growth, 2004, 271, 274-286.	1.5	13
81	In Situ Electrochemical X-ray Spectromicroscopy Investigation of the Reduction/Reoxidation Dynamics of Ni–Cu Solid Oxide Fuel Cell Anodic Material in Contact with a Cr Interconnect in 2 × 10 <sup>–6</sup> mbar O <sub>2</sub> . Journal of Physical Chemistry C, 2012, 116, 7243-7248.	3.1	13
82	Novel insight into bronze disease gained by synchrotron-based photoelectron spectro-microscopy, in support of electrochemical treatment strategies. Studies in Conservation, 2017, 62, 465-473.	1.1	13
83	Preparation of InAs by annealing of two-layer In–As electrodeposits. Journal of Alloys and Compounds, 2004, 366, 152-160.	5.5	12
84	An SFG and ERS investigation of the corrosion of CoW0.013C0.001 alloys and WC–Co cermets in CNâ^'-containing aqueous solutions. Corrosion Science, 2007, 49, 2392-2405.	6.6	12
85	An investigation of the corrosion of WC–Co cermets in CNâ^'-containing aqueous solutions. Part II: Synchrotron-based high lateral-resolution XPS study. Corrosion Science, 2009, 51, 1675-1678.	6.6	12
86	Cathodic chloride extraction treatment of a late bronze-age artifact affected by bronze disease in room-temperature ionic-liquid 1-ethyl-3-methylimidazolium bis(trifluoromethanesulfonyl)imide (EMI-TFSI). Journal of Solid State Electrochemistry, 2010, 14, 479-494.	2.5	12
87	Microscale Evolution of Surface Chemistry and Morphology of the Key Components in Operating Hydrocarbon-Fuelled SOFCs. Journal of Physical Chemistry C, 2012, 116, 23188-23193.	3.1	12
88	Spectroelectrochemical study of the electro-oxidation of ethanol on WC-supported Pt – Part III: Monitoring of electrodeposited Pt catalyst ageing by in situ Fourier transform infrared spectroscopy, in situ sum frequency generation spectroscopy and ex situ photoelectron spectromicroscopy. Journal of Power Sources, 2013, 231, 6-17.	7.8	12
89	In situ near-ambient pressure X-ray photoelectron spectroscopy discloses the surface composition of operating NdBaCo2O5+1´ solid oxide fuel cell cathodes. Journal of Power Sources, 2019, 436, 226815.	7.8	12
90	An Erosion-Corrosion Investigation of Coated Steel for Applications in the Oil and Gas Field, Based on Bipolar Electrochemistry. Coatings, 2020, 10, 92.	2.6	12

#	Article	IF	CITATIONS
91	On the observation of inductive high-frequency impedance behaviour during the electrodeposition of Au–Sn alloys. Journal of Applied Electrochemistry, 2004, 34, 277-281.	2.9	11
92	A class of mathematical models for alternated-current electrochemical measurements accounting for non-linear effects. Nonlinear Analysis: Real World Applications, 2008, 9, 412-429.	1.7	11
93	Study of a proton exchange membrane fuel cells catalyst subjected to anodic operating conditions, by synchrotron-based scanning photoelectron microscopy (SPEM) and high lateral-resolution X-ray photoelectron spectroscopy. Journal of Power Sources, 2011, 196, 2513-2518.	7.8	11
94	Electrochemical reconstruction of a heavily corroded Tarentum hemiobolus silver coin: a study based on microfocus X-ray computed microtomography. Journal of Archaeological Science, 2014, 52, 24-30.	2.4	11
95	Spiral waves on the sphere for an alloy electrodeposition model. Communications in Nonlinear Science and Numerical Simulation, 2019, 79, 104930.	3.3	11
96	The role of chromium in the corrosion performance of cobalt- and cobalt-nickel based hardmetal binders: A study centred on X-ray absorption microspectroscopy. International Journal of Refractory Metals and Hard Materials, 2020, 92, 105320.	3.8	11
97	An SFG and DFG investigation of polycrystalline Au, Au–Cu and Au–Ag–Cu electrodes in contact with aqueous solutions containing KCN. Journal of Alloys and Compounds, 2007, 427, 341-349.	5.5	10
98	A SERS investigation of the electrodeposition of Au in a phosphate solution. Surface and Coatings Technology, 2007, 201, 6267-6272.	4.8	10
99	An SFG and DFG investigation of Au(111), Au(100), Au(110) and Au(210) electrodes in contact with aqueous solutions containing KCN. Journal of Solid State Electrochemistry, 2008, 12, 303-313.	2.5	10
100	Electrodeposition of NiO/YSZ from hydroalcoholic solutions containing Chitosan. Surface and Coatings Technology, 2009, 203, 3427-3434.	4.8	10
101	A SERS study of the galvanostatic sequence used for the electrochemical deposition of copper from baths employed in the fabrication of interconnects. Journal of Materials Science: Materials in Electronics, 2009, 20, 217-222.	2.2	10
102	In Situ Electrochemical SFG/DFG Study of CNâ^' and Nitrile Adsorption at Au from 1-Butyl-1-methyl-pyrrolidinium Bis(trifluoromethylsulfonyl) Amide Ionic Liquid ([BMP][TFSA]) Containing 4-{2-[1-(2-Cyanoethyl)-1,2,3,4-tetrahydroquinolin-6-yl]diazenyl} Benzonitrile (CTDB) and K[Au(CN)2]. Molecules, 2012, 17, 7722-7736.	3.8	10
103	Morphochemical evolution during ageing of pyrolysed Mn/polypyrrole nanocomposite oxygen reduction electrocatalysts: A study based on quasi-in situ photoelectron spectromicroscopy. Journal of Electroanalytical Chemistry, 2015, 758, 191-200.	3.8	10
104	<i>In situ</i> observation of dynamic electrodeposition processes by soft x-ray fluorescence microspectroscopy and keyhole coherent diffractive imaging. Journal Physics D: Applied Physics, 2017, 50, 124001.	2.8	10
105	Soft X-ray ptychography as a tool for in operando morphochemical studies of electrodeposition processes with nanometric lateral resolution. Journal of Electron Spectroscopy and Related Phenomena, 2017, 220, 147-155.	1.7	10
106	Silver electrodeposition from water–acetonitrile mixed solvents in the presence of tetrabutylammonium perchlorate. Journal of Solid State Electrochemistry, 2009, 13, 1553-1559.	2.5	9
107	Numerical approximation of oscillating Turing patterns in a reaction-diffusion model for electrochemical material growth. AIP Conference Proceedings, 2012, , .	0.4	9
108	In situ SERS and ERS assessment of the effect of triethanolamine on zinc electrodeposition on a gold electrode. Electrochimica Acta, 2017, 248, 270-280.	5.2	9

#	Article	IF	CITATIONS
109	Morphological Artefacts in EDX Analyses of Electrodeposited Zn-Mn Films. Transactions of the Institute of Metal Finishing, 2000, 78, 93-95.	1.3	8
110	A Mathematical Model for the Corrosion of Metallic Bipolar Plates in PEM Fuel Cells: Numerical and Experimental Issues. SIAM Journal on Applied Mathematics, 2009, 70, 579-599.	1.8	8
111	Scanning photoelectron microscopy investigation of the initial stages of the electrochemical reduction of Cr(VI) at Pt(111) electrode. Journal of Electroanalytical Chemistry, 2011, 657, 113-116.	3.8	8
112	Electrodeposition of Ni/ceria composites: an in situ visible reflectance investigation. Journal of Solid State Electrochemistry, 2012, 16, 3429-3441.	2.5	8
113	An in situ near-ambient pressure X-ray photoelectron spectroscopy study of CO 2 reduction at Cu in a SOE cell. Journal of Electroanalytical Chemistry, 2017, 799, 17-25.	3.8	8
114	XRF map identification problems based on a PDE electrodeposition model. Journal Physics D: Applied Physics, 2017, 50, 154002.	2.8	8
115	Operando soft Xâ€ray microscope study of rechargeable Zn–air battery anodes in deep eutectic solvent electrolyte. X-Ray Spectrometry, 2019, 48, 527-535.	1.4	8
116	Electrodeposition of Zinc from Alkaline Electrolytes Containing Quaternary Ammonium Salts and Ionomers: Impact of Cathodicâ€Anodic Cycling Conditions. ChemElectroChem, 2020, 7, 1752-1764.	3.4	8
117	Ultrafast Charge Carrier Dynamics in CuWO <sub>4</sub> Photoanodes. Journal of Physical Chemistry C, 2021, 125, 5692-5699.	3.1	8
118	Corrosion Performance of Austenitic Stainless Steel Bipolar Plates for Nafion- and Room-Temperature Ionic-Liquid-Based PEMFCs. Open Fuels and Energy Science Journal, 2012, 5, 47-52.	0.2	8
119	Electrodeposition of copper from triethanolamine as a complexing agent in alkaline solution. Electrochimica Acta, 2022, 425, 140654.	5.2	8
120	Metastable structures in electrodeposited AuCu. Scripta Materialia, 2000, 43, 877-880.	5.2	7
121	Study of Surface Compositional Waves in Electrodeposited Au–Cu Alloys by Synchrotron-Based High Lateral-Resolution X-Ray Photoemission Spectroscopy. Journal of the Electrochemical Society, 2008, 155, F165.	2.9	7
122	In situ spectroelectrochemical measurements during the electro-oxidation of ethanol on WC-supported Pt-black. Part II: Monitoring of catalyst aging by in situ Fourier transform infrared spectroscopy. Journal of Power Sources, 2010, 195, 7968-7973.	7.8	7
123	Electrochemical fabrication of nanoporous gold decorated with manganese oxide nanowires from eutectic urea/choline chloride ionic liquid. Part II – Electrodeposition of Au–Mn: A study based on soft X-ray microspectroscopy. Electrochimica Acta, 2013, 114, 889-896.	5.2	7
124	Parameter identification in ODE models with oscillatory dynamics: a Fourier regularization approach. Inverse Problems, 2017, 33, 124009.	2.0	7
125	Depth-Dependent Scanning Photoelectron Microspectroscopy Unravels the Mechanism of Dynamic Pattern Formation in Alloy Electrodeposition. Journal of Physical Chemistry C, 2018, 122, 15996-16007.	3.1	7
126	Formation of GaAs by annealing of two-layer Ga-As electrodeposits. Journal of Alloys and Compounds, 2004, 379, 209-215.	5.5	6

8

#	Article	IF	CITATIONS
127	Electrodeposition of a Au-Dy2O3 Composite Solid Oxide Fuel Cell Catalyst from Eutectic Urea/Choline Chloride Ionic Liquid. Energies, 2012, 5, 5363-5371.	3.1	6
128	Electrodeposition of Y2O3–Au composite coatings for SOFC interconnects:in situmonitoring of film growth by surface enhanced Raman spectroscopy. Transactions of the Institute of Metal Finishing, 2012, 90, 30-37.	1.3	6
129	Operando XAS of a Bifunctional Gas Diffusion Electrode for Zn-Air Batteries under Realistic Application Conditions. Applied Sciences (Switzerland), 2021, 11, 11672.	2.5	6
130	In situ femtosecond spectroelectrochemistry of Au(111) in an aqueous chloride solution. Electrochemistry Communications, 2009, 11, 799-803.	4.7	5
131	A SERS investigation of Cu electrodeposition in the presence of the model leveller 4-{2-[1-(2-cyanoethyl)-1,2,3,4-tetrahydroquinolin-6-yl]diazenyl} benzonitrile. Electrochimica Acta, 2010, 55, 3279-3285.	5.2	5
132	In SituSoft X-ray Microscopy Study of Fe Interconnect Corrosion in Ionic Liquid-Based Nano-PEMFC Half-Cells. Fuel Cells, 2013, 13, 196-202.	2.4	5
133	Electrodeposition of DLC films on carbon steel from acetic acid solutions. Transactions of the Institute of Metal Finishing, 2014, 92, 183-188.	1.3	5
134	Accurate Assessment of the Oxygen Reduction Electrocatalytic Activity of Mn/Polypyrrole Nanocomposites Based on Rotating Disk Electrode Measurements, Complemented with Multitechnique Structural Characterizations. Journal of Analytical Methods in Chemistry, 2016, 2016, 1-16.	1.6	5
135	Dy- and Tb-doped CeO2-Ni cermets for solid oxide fuel cell anodes: electrochemical fabrication, structural characterization, and electrocatalytic performance. Journal of Solid State Electrochemistry, 2018, 22, 3761-3773.	2.5	5
136	Monitoring dynamic electrochemical processes with in situ ptychography. Applied Nanoscience (Switzerland), 2018, 8, 627-636.	3.1	5
137	X-ray imaging and micro-spectroscopy unravel the role of zincate and zinc oxide in the cycling of zinc anodes in mildly acidic aqueous electrolytes. Journal of Power Sources, 2022, 524, 231063.	7.8	5
138	Silver coated lead coins: An appraisal of ancient technology. Journal of Applied Electrochemistry, 2006, 36, 951-956.	2.9	4
139	SFG and DFG investigation of Au(111), Au(210), polycrystalline Au, Au–Cu and Au–Ag–Cu electrodes in contact with aqueous solutions containing KCN and 4-cyanopyridine. Journal of Applied Electrochemistry, 2008, 38, 897-906.	2.9	4
140	Corrosion of stainless steel grades in molten NaOH/KOH eutectic at 250 °C: AISI304 austenitic and 2205 duplex. Materials and Corrosion - Werkstoffe Und Korrosion, 2012, 63, n/a-n/a.	1.5	4
141	Electrodeposition of a Mn–Cu–ZnO Hybrid Material for Supercapacitors: A Soft Xâ€ray Fluorescence and Absorption Microspectroscopy Study. ChemElectroChem, 2014, 1, 392-399.	3.4	4
142	Potential-dependent reactivity of adsorbed cyanide during the electrodeposition of silver from cyanocomplexes: a study based onin-situsurface-enhanced Raman spectroscopy. Transactions of the Institute of Metal Finishing, 2015, 93, 82-88.	1.3	4
143	Insight into the Cycling Behaviour of Metal Anodes, Enabled by Xâ€ <b>r</b> ay Tomography and Mathematical Modelling. ChemElectroChem, 2022, 9, .	3.4	4
144	Single Metal Atom Catalysts and ORR: H-Bonding, Solvation, and the Elusive Hydroperoxyl Intermediate. ACS Catalysis, 2022, 12, 7950-7959.	11.2	4

#	Article	IF	CITATIONS
145	Silver electrodeposition from water–acetonitrile mixed solvents. Part Ill—an in situ investigation by optical second harmonic generation spectroscopy. Journal of Solid State Electrochemistry, 2010, 14, 989-995.	2.5	3
146	Unusual coin from the Parabita hoard: combined use of surface and micro-analytical techniques for its characterisation. Journal of Cultural Heritage, 2010, 11, 233-238.	3.3	3
147	Wireless system for biological signal recording with Gallium Arsenide high electron mobility transistors as sensing elements. Microelectronic Engineering, 2013, 111, 354-359.	2.4	3
148	A comprehensive assessment of the performance of corrosion resistant alloys in hot acidic brines for application in oil and gas production. Corrosion Engineering Science and Technology, 2017, 52, 99-113.	1.4	3
149	Spatially Resolved XPS Characterization of Electrochemical Surfaces. Surfaces, 2019, 2, 295-314.	2.3	3
150	Anodic behaviour of amorphous NiP/tin multilayers in an acidic chloride solution. Corrosion Science, 2003, 45, 1161-1171.	6.6	2
151	Electrodeposition of NiFe Alloys in a Magnetic Field. ECS Transactions, 2007, 3, 15-27.	0.5	2
152	Turing Instability in an Electrodeposition Morphogenesis Model: An Analytical, Numerical and Experimental Study. AIP Conference Proceedings, 2007, , .	0.4	2
153	A computational approach to morphological control in electrodeposition by molecular targeting. Computational Materials Science, 2008, 42, 394-406.	3.0	2
154	Corrosion of electrodeposited copper by exposure to volatile organic compounds. Journal of Materials Science: Materials in Electronics, 2009, 20, 666-670.	2.2	2
155	Corrosion of stainless steel grades in H2 O/KOH 50% at 120 °C: AISI304 austenitic and 2205 duplex. Materials and Corrosion - Werkstoffe Und Korrosion, 2013, 64, 988-995.	1.5	2
156	Pulseâ€Plating of Mn–Cu–ZnO for Supercapacitors: A Study Based on Soft Xâ€ray Fluorescence and Absorption Microspectroscopy. ChemElectroChem, 2014, 1, 1161-1172.	3.4	2
157	Turing-Hopf patterns in a morphochemical model for electrodeposition with cross-diffusion. Applications in Engineering Science, 2021, 5, 100034.	0.8	2
158	Model-reduction techniques for PDE models with Turing type electrochemical phase formation dynamics. Applications in Engineering Science, 2021, 8, 100074.	0.8	2
159	A tribological study of electrodeposited gold-copper-cadmium. Metal Finishing, 2003, 101, 42-47.	0.0	1
160	Materials science aspects of zincâ $\in$ "air batteries: a review. , 2014, 3, 1.		1
161	Quantifying and rationalizing polarization curves of Zn-air fuel-cells: A simple enabling contribution to device-scale analysis and monitoring. Electrochimica Acta, 2022, 425, 140712.	5.2	1
162	A STM Investigation on Step Dynamics during Cu Electrodeposition. Part I - Development of the Electrolyte ECS Transactions, 2009, 16, 37-52.	0.5	0

#	Article	IF	CITATIONS
163	A novel selective removal process of cobalt silicide. Journal of Materials Science: Materials in Electronics, 2009, 20, 1164-1171.	2.2	0
164	In situ photoelectron spectromicroscopy for the investigation of solid oxide–based electrochemical systems. , 2020, , 55-89.		0
165	Fourier analysis of an electrochemical phase formation model enables the rationalization of zinc-anode battery dynamics. Applications in Engineering Science, 2021, 5, 100033.	0.8	0